


Received December 2, 2017, accepted January 7, 2018, date of publication January 23, 2018, date of current version March 16, 2018.

Digital Object Identifier 10.1109/ACCESS.2018.2796082

A Closed-Form and Stochastic Wall Insertion Loss Model for Dense Small Cell Networks

YANG LIU¹ , YU YU², QIONG WU¹, ZHENG-QUAN LI¹, WEN-JUN LU² , (Member, IEEE),
AND HONG-BO ZHU²

¹School of IoT Engineering, Jiangnan University, Wuxi 214122, China

²Nanjing University of Posts and Telecommunications, Nanjing 210003, China

Corresponding author: Yang Liu (ly71354@163.com)

This work was supported in part by National Nature Science Foundation Council Proposal under Grant 61427801, Grant 61471204, and Grant 61571108, in part by the Open Foundation of Key Laboratory of Wireless Communication, Nanjing University of Posts and Telecommunication, under Grant 2017WICOM01, and in part by the Fundamental Research Funds for the Central Universities under Grant JUSRP11738 and Grant JUSRP11742.

ABSTRACT A novel closed-form and stochastic internal wall insertion loss model (IWIL) in the indoor-indoor channel is proposed in this paper. The IWIL (dimensionless) is modeled as a generalized beta prime distributed random variable on the basis of the Nakagami fading. The probability distribution function (PDF), expectation, and standard deviation of IWIL are derived based on the proposed model. The impacts of the Nakagami-m parameters on the expectation and standard deviation of IWIL are also analyzed. Extensive IWIL measurements at 3.5, 6, and 11 GHz are carried out to validate the proposed model. Both Kolmogorov-Smirnov and Chi-square tests are exploited to determine the goodness of fitting between the modeled and measured data. Results show that the modeled PDF provides a better fit to the measured PDF than that of the Log-normal distribution. The proposed model can be used for the dense small cell networks in the future fifth generation wireless communication.

INDEX TERMS Wall insertion loss, generalized beta prime distribution, dense small cell networks, K-S test, Chi-square test.

I. INTRODUCTION

The emerging fifth generation (5G) wireless communication system may be commonly deployed around 2020 to provide high transmission rates and spectral efficiency [1]. The dense small cell is assumed to be one of the key technologies in the future 5G communication system [2]. However, this technology involves an indoor-indoor scenario and traditional outdoor-outdoor or outdoor-indoor channel models are no longer adequate in this scenario. Thus, accurate description of the indoor-indoor channel is essentially important for designing and evaluating the dense small cell networks.

The propagation characteristics of the indoor-indoor channel have been intensively studied since 1987 [3]. Parameters such as the path loss [4]–[6], root mean square delay spread [7]–[9], small scale fading [10]–[12], and power delay profiles [13]–[15] are intensively studied. As one of the typical parameters in the indoor-indoor channel, the internal wall insertion loss (IWIL) also plays an important role in the communication system design, like the dense small cell planning, wireless coverage prediction and electromagnetic

compatibility analysis. Therefore, it is necessary to study IWIL for the future communication design.

In the past decades, certain research about the IWIL has been reported in the indoor-indoor channel [16]–[18]. Generally, they can be categorized into two distinctive types. The first type is the material dependency. The IWIL for several materials, such as glass, wood, brick, metal has been measured [16]–[17]. Results show that the metal yields the largest IWIL and the glass yields the least. The second type is the thickness dependency [17], [18]. Attenuation caused by the internal walls with different thicknesses has been measured. Results indicate that there is an almost linear rise of attenuation with the thickness.

Basically, the above studies focus on the expectation of IWIL in the indoor-indoor channel. However, the other statistical properties such as the distribution of IWIL are not taken into account. Actually, small-scale fading might introduce significant fluctuations in IWIL. To obtain better accuracy in radio link budget or wireless coverage estimation in dense small cell networks, a more accurate IWIL with better

generality is essential. Motivated by this reason, a novel generalized beta prime distributed IWIL model is proposed in this paper. The probability distribution function (PDF) of IWIL in the indoor-indoor channel with Nakagami fading is derived. In addition, the closed-form formulas for the expectation and standard deviation of IWIL are also provided. The impacts of Nakagami-m parameters on the expectation and standard deviation are studied and analyzed. The accuracy of the proposed model is validated by the extensive IWIL measurements in three different office buildings at 3.5GHz (S band), 6GHz (C band), 11GHz (X band). The goodness of fitting between the measured and modeled results is determined by the Kolmogorov-Smirnov (K-S) and Chi-square tests.

II. CLOSED-FORM STATISTICAL MODEL

In this section, a novel statistical IWIL model based on the Nakagami fading theory is proposed. The presented model focuses on the statistical properties of IWIL. Therefore, our considerations are restricted to the stationary and frequency-non-selective channel.

A. CLOSED-FORM MODEL

The IWIL (dimensionless) is defined as the ratio of the instantaneous power in the absence of the wall (abs-link) to that in the presence of the wall (pre-link) [19].

In a Nakagami fading channel, both of the signal amplitudes in the pre-link and abs-link, are Nakagami distributed [20], shown as,

$$s_{abs} \sim Nakagami(m_1, \Omega_1) \tag{1}$$

$$s_{pre} \sim Nakagami(m_2, \Omega_2) \tag{2}$$

with

$$m_1 = E^2(s_{abs}^2)/Var(s_{abs}^2) \tag{3}$$

$$\Omega_1 = E(s_{abs}^2) \tag{4}$$

$$m_2 = E^2(s_{pre}^2)/Var(s_{pre}^2) \tag{5}$$

$$\Omega_2 = E(s_{pre}^2) \tag{6}$$

where s_{abs} and s_{pre} are the amplitudes of the signals in the pre-link and abs-link, respectively. $E(\cdot)$ and $Var(\cdot)$ denote the expectation and variance of a random variable, respectively. The parameter m_1 is the shape factor of the abs-link representing the severity of fading. The large m_1 is, the less amount of fading is present in the abs-link. The parameter Ω_1 represents the mean power of the abs-link. The parameters m_2 and Ω_2 are similarly defined for the pre-link.

If the amplitude possesses a Nakagami distribution with parameters m_1 and Ω_1 , the corresponding power has a Gamma distribution with a shape parameter m_1 and a scale parameter Ω_1/m_1 [14]. Hence, we have

$$s_{abs}^2 \sim Gamma(m_1, \Omega_1/m_1) \tag{7}$$

where the P_{abs} is the received power in the abs-link.

Similarly, the received power in the pre-link is also gamma distributed with shape m_2 and scale Ω_2/m_2 , shown as,

$$s_{pre}^2 \sim Gamma(m_2, \Omega_2/m_2) \tag{8}$$

where the P_{pre} is the received power in the pre-link.

Then, the IWIL, I_{loss} , can be calculated as

$$I_{loss} = \frac{s_{abs}^2}{s_{pre}^2} \tag{9}$$

The generalized beta prime distribution can be used to model the IWIL [21]. The PDF of the IWIL can be shown as (see the proof in the Appendix A)

$$f_{I_{loss}}(x) = \frac{(x \cdot \frac{\Omega_2}{\Omega_1} \cdot \frac{m_1}{m_2})^{m_1-1} (1 + x \cdot \frac{\Omega_2}{\Omega_1} \cdot \frac{m_1}{m_2})^{-m_1-m_2}}{\frac{\Omega_2}{\Omega_1} \cdot \frac{m_2}{m_1} B(m_1, m_2)} \tag{10}$$

where B is the Beta function [22]

In this proposed model, the m-factors in the abs-link and pre-link, m_1, m_2 , the mean power of the abs-link and pre-link, Ω_1, Ω_2 , are needed to be extracted. These parameters can be obtained according to (3)-(6).

B. STATISTICAL PARAMETER ANALYSIS

Based on the proposed model, the expectation and standard deviation of the IWIL can be derived as(see the proof in the Appendix B),

$$E(I_{loss}) = \frac{\Omega_1}{\Omega_2} \cdot \frac{m_2}{m_2 - 1} \quad m_2 > 1 \tag{11}$$

$$Std(I_{loss}) = \frac{m_2}{m_1} \cdot \frac{\Omega_1}{\Omega_2} \sqrt{\frac{m_1(m_1 + m_2 - 1)}{(m_2 - 2)(m_2 - 1)^2}} \quad m_2 > 2 \tag{12}$$

where $E(I_{loss})$ and $Std(I_{loss})$ are the expectation and standard deviation of IWIL respectively. The conditions on the shape factor of the pre-link in (11) and (12) are necessary since the expectation and standard deviation are not existed when these conditions are not satisfied.

Then, the influences of m-factors on the statistical behaviour of IWIL are studied as follows if the expectation and standard deviation of IWIL exist.

Equation (11) indicates that the expectation of IWIL depends on not only the ratio of the mean powers of the abs-link and pre-link, Ω_1/Ω_2 , but also the shape factor of the pre-link, m_2 . The expectations of IWIL as a function of m_2 are shown in Fig.1 (IWIL has been converted into decibel). The expectations decrease as the m_2 -factor increases for a constant Ω_1/Ω_2 and it tends to Ω_1/Ω_2 for large m_2 -factor. This can be explained as m_2 -factor increases, the received signal in the pre-link fluctuated slightly, thus the mean IWIL tends to the ratio of the mean power in the abs-link and in the pre-link. On the other hand, when m_2 -factor tends to 1, the expectation of IWIL tends to infinity. The reason is that when m_2 -factor tends to 1, Nakagami degrades into Rayleigh fading, leading to the unstable IWIL and the non-convergence of the expectation.

It can be directly seen that the standard deviation of IWIL is in proportion to Ω_1/Ω_2 from equation (12). The effects

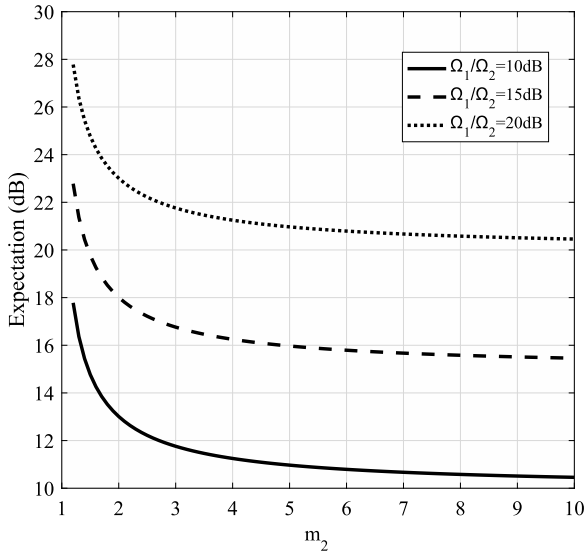


FIGURE 1. The expectation of the wall insertion loss as a function of m_2 .

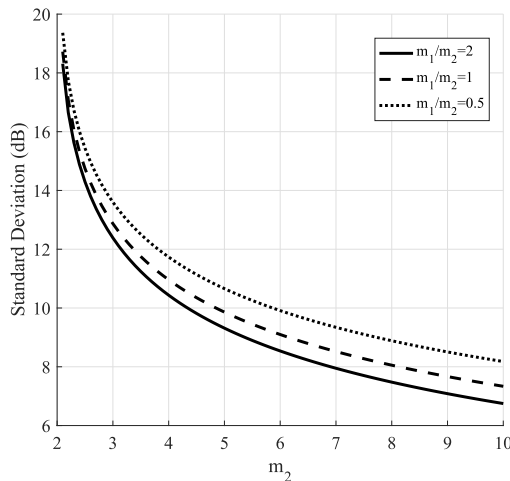


FIGURE 2. The standard deviation of the wall insertion loss as a function of m_2 .

of m_1 and m_2 on the standard deviation with $\Omega_1/\Omega_2 = 10dB$ are depicted in Fig.2. The ratio of the shape factors of the abs-link and pre-link, m_1/m_2 , is selected as 0.5, 1, 2 respectively. For a fixed m_1/m_2 , the standard deviation decreases as the m-factors of both links increase, owing to the fluctuations of the signals becoming slighter when both of the m-factors in the abs-link and pre-link tend to infinity.

III. MEASUREMENT SETUP

In order to validate the proposed model, extensive IWIL measurements are carried out at 3.5GHz, 6GHz and 11GHz. Besides, two combinations of the antennas' polarizations are considered to confirm the proposed model sufficiently. If V is defined as the vertical polarization and H is defined as the horizontal polarization, the two combinations are V-V and V-H, where the first letter is for the transmitted (Tx) antenna and the second is for the received (Rx) antenna.

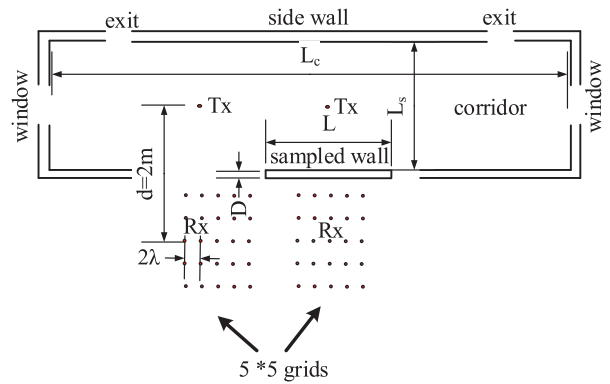


FIGURE 3. The diagrammatic sketch of the measurement environment and setup.

TABLE 1. The parameters of the measurement environment and the sampled walls.

building	material	$L_c(m)$	$L_s(m)$	D(m)	L(m)	h(m)
building1	Concrete	48	4.6	0.16	8.6	2.8
building2	Concrete	32	3.9	0.17	3.3	2.8
building3	Concrete	43	4.3	0.19	7.4	3.1

A. MEASUREMENT ENVIRONMENT

The measurements are performed at three corridors with length of 32m-48m (L_c) in three different office buildings. The distances between the side walls and the sampled walls, L_s , range from 5.9m-6.6m, as depicted in Fig.3. There are two windows at the east and west side of each corridor. The sampled walls span from the floors to the ceilings. The walls under test are made of the reinforced concrete, which is a typical building material. The thicknesses (D) of the walls range from 16cm-19cm. The heights (h) and the widths (L) of the sampled walls are 2.8m-3.1m and 3.3m-8.6m respectively. The diffracted and reflected waves by the edge of the sampled walls, the side walls and the windows have little influence on the IWIL [23]. The furniture and the other objects (such as the dustbins) are removed during the measurement. The parameters of the measurement environments and the sampled walls are summarized in Table 1.

B. MEASUREMENT SYSTEM

The block diagram of the IWIL measurement system conducted by the Agilent 8720ET vector network analyzer (VNA) is shown in Fig. 4 [23], [24]. Three different 10-dBm, 201-point sweeping signals from 3490-3510 MHz, 5990-6010 MHz, 10990-11010 MHz are generated by the VNA. The received signal is sent back to the VNA via a 15m-long coaxial cable. Both the Tx and Rx antennas are omnidirectional monopoles with a gain of 3 dBi. During the measurements, both of the Tx and Rx antennas are mounted on the wooden tripods with a height of 1.5m above the floor. The laptop computer is used to store the complex frequency response data through a GPIB interface. The measurement system is calibrated before conducting the measurement.

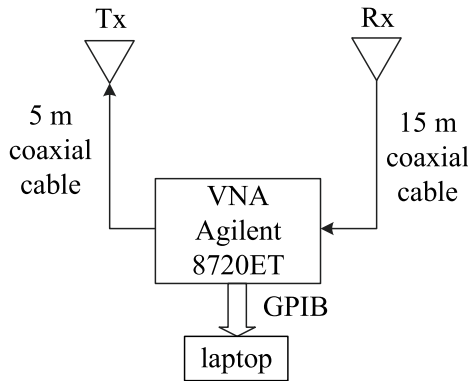


FIGURE 4. Block diagram of the measurement system.

TABLE 2. The parameters of the IWIL measurement system.

Center frequency	3GHz, 6GHz, 11GHz	
bandwidth	20MHz	
Sweeping points	201	
power	10dBm	
Tx feeder	length	attenuation
	5m	0.6dB/m
Rx feeder	length	attenuation
	15m	0.6dB/m
Tx antenna gain	3dBi	
Rx antenna gain	3dBi	
antenna height	1.5m	

The parameters of the measurement system are summarized in Table 2.

C. MEASUREMENT PROCEDURE

The received signal in the absence of wall is measured to establish a reference. Then the Tx and Rx antennas are placed on the opposite sides of the sampled wall with the same Tx-Rx distance of the reference measurement. The sampled wall is located at the midpoint of the Tx-Rx antennas. The distance between the Tx and Rx antennas (d) is set to be 2m (larger than ten wavelengths) so that the sampled walls are in the far field of the Tx and Rx antennas. In this arrangement, the electromagnetic wave incident on the sampled walls is essentially a plane wave [23]. In order to study the fluctuation of IWIL caused by the small-scale variations of the terminals, both measurements are conducted at 5×5 grids with an interval of 2λ . Both measurements are repeated 8 times for one grid.

IV. PERFORMANCE OF THE PROPOSED IWIL MODEL

The sampled IWIL is computed from (9) by the measured complex frequency responses.

The parameters of the proposed model, $m_1, m_2, \Omega_1, \Omega_2$, estimated from the measured data according to (3)-(6) are summarized in the Table 3-5. Then the modeled PDF of the IWIL can be obtained from (10). All the parameters for each sampled wall, frequency and polarization are estimated based on the complex frequency response samples over the 25-point grid, 8 temporal bins and 201 frequency points. From the Table 3-5, it can be seen that the estimated m-factors are

TABLE 3. The parameters of the proposed model estimated from the measured data at 3.5GHz.

building	V-V			V-H		
	m_1	m_2	Ω_1/Ω_2	m_1	m_2	Ω_1/Ω_2
building1	1.39	1.39	80.2	2.1	1.3	60.6
building2	3.03	1.28	58.0	1.33	1.76	38.5
building3	1.36	1.13	38.2	1.40	1.43	38.2

TABLE 4. The parameters of the proposed model estimated from the measured data at 6GHz.

building	V-V			V-H		
	m_1	m_2	Ω_1/Ω_2	m_1	m_2	Ω_1/Ω_2
building1	1.6	2.09	84.3	1.09	1.29	81.2
building2	2.21	1.33	113.7	1.33	1.16	77.4
building3	2.13	1.79	91.5	2.09	1.27	76.3

TABLE 5. The parameters of the proposed model estimated from the measured data at 11GHz.

building	V-V			V-H		
	m_1	m_2	Ω_1/Ω_2	m_1	m_2	Ω_1/Ω_2
building1	1.34	1.26	353.6	1.26	1.14	233.3
building2	1.53	1.35	495.1	1.17	1.1	189.3
building3	2.62	1.64	372.7	1.11	1.08	170.7

TABLE 6. The expectations of IWIL for different polarizations at 3.5GHz 6GHz 11GHz.

building	V-V			V-H		
	3.5GHz	6GHz	11GHz	3.5GHz	6GHz	11GHz
building1	24.0dB	24.1dB	31.6dB	26.0dB	26.7dB	31.1dB
building2	23.7dB	27.6dB	31.5dB	19.4dB	27.8dB	32.8dB
building3	24.0dB	23.2dB	31.0dB	21.3dB	24.0dB	34.2dB

larger than 1 whether in a line-of-sight or none-line-of-sight channel. This is determined by the propagation properties of the indoor-indoor channel. The waveguide effects in the indoor propagation environment lead to the fading less severe than a Rayleigh fading. Thus, the expectation of IWIL exists in the indoor-indoor channel.

A. EXPECTATION OF THE IWIL FOR EACH FREQUENCY

The expectations of IWIL for different polarizations at 3.5GHz, 6GHz and 11GHz are shown in Table 6. The mean IWIL is computed by the estimator

$$\widehat{IL}_{loss} = N^{-1} \sum_{i=1}^N IL_{loss}^i \quad (13)$$

IL_{loss}^i denotes the i^{th} IWIL sample and N shows the number of samples. In practice, this expectation estimator based on the law of large number [25] is widely used when the corresponding distribution has a convergent expectation.

Then this estimator is employed to determine the accuracy of the modeled mean IWIL. The measured mean IWIL estimated from (13) is compared with the modeled expectation computed from (11), as shown in Fig. 5. In this figure, each circle corresponds to the measured mean IWIL for each of the buildings, frequencies and polarizations. The diagonal line indicates no error between the measured and modeled mean IWIL. Fig. 5 shows that the modeled mean IWIL

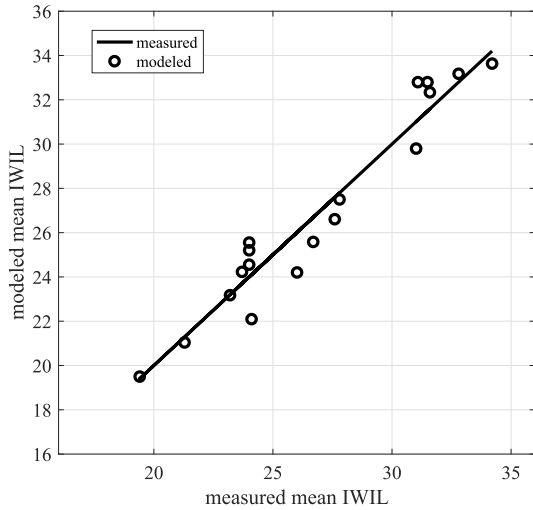


FIGURE 5. Measured mean IWIL compared with modeled IWIL. The diagonal line corresponds to no modeled error.

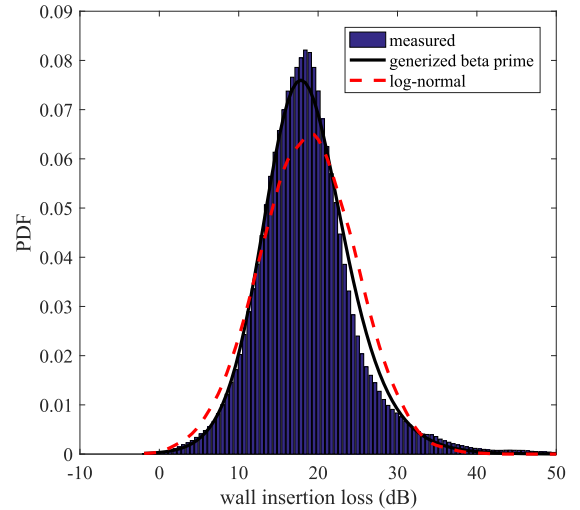


FIGURE 7. The modeled and the measured PDF of the wall insertion loss for V-H polarization at 3.5GHz in building1.

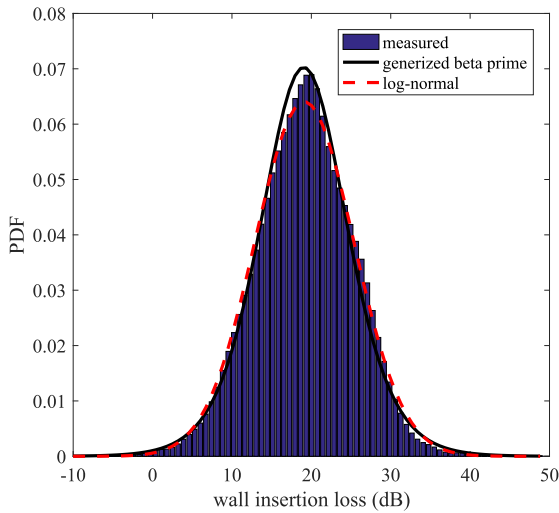


FIGURE 6. The modeled and the measured PDF of the wall insertion loss for V-V polarization at 3.5GHz in building1.

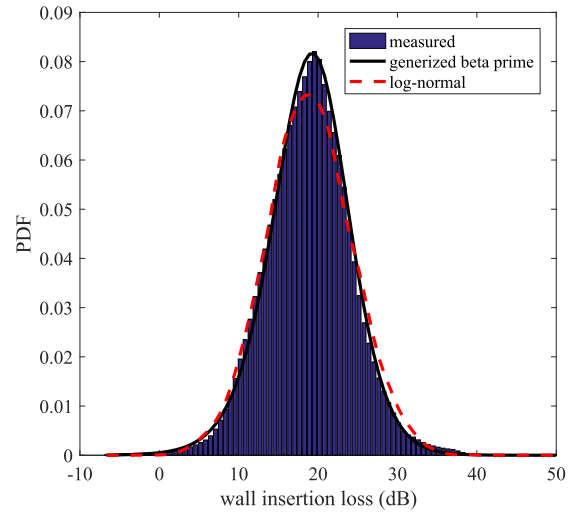


FIGURE 8. The modeled and the measured PDF of the wall insertion loss for V-V polarization at 6GHz in building1.

approximates the measured results (± 2 dB, the small difference between the measured and modeled IWIL is caused by the measurement error such as the measured noise, the limited number of the measured samples), proving that the modeled IWIL is accurate.

The results in Table 6 show a significant trend for an increase in the IWIL as the frequency increases, due to the fact that the ratio of the mean powers in the abs-link and in the pre-link, Ω_1/Ω_2 , shows an increased trend for the higher frequency as seen in the Table 3-5.

B. K-S AND CHI-SQUARE TEST FOR THE PROPOSED IWIL MODEL

Next, the empirical PDF of the measured IWIL are compared with the modeled PDF for each frequency and polarizations, as shown in Fig. 6-11 (These figures only describe the

comparisons in building1). The PDFs of Log-normal distribution are also depicted in these figures for comparisons. The Log-normal distribution is defined as a continuous distribution with a random variable whose logarithm is normally distributed, shown in the following [26]

$$f_Y(y) = \frac{1}{y} \cdot \frac{1}{\sigma\sqrt{2\pi}} \exp\left(-\frac{(\ln y - \mu)^2}{2\sigma^2}\right) \quad (14)$$

where σ and μ are the parameters of the Log-normal distribution.

As seen in these figures, the proposed model matches better with the measured data than the Log-normal distribution.

In order to give a scientific quantification of the goodness of the fit between the measurements and proposed model, both Kolmogorov-Smirnov (K-S) [27] and Chi-square tests [28] are exploited.

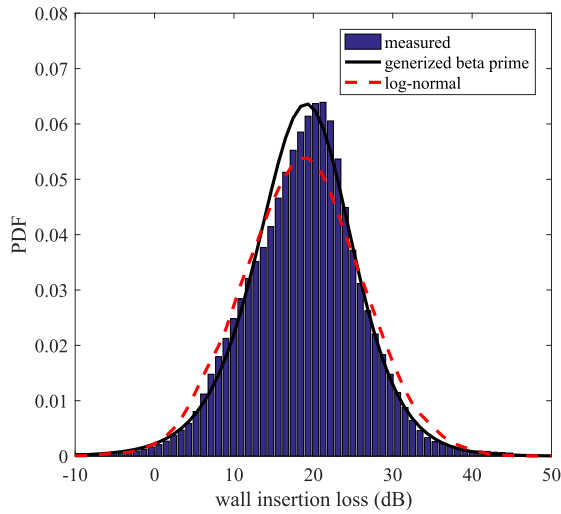


FIGURE 9. The modeled and the measured PDF of the wall insertion loss for V-H polarization at 6GHz in building1.

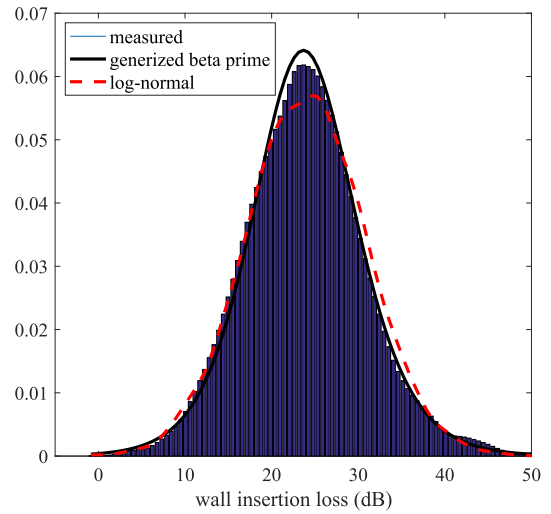


FIGURE 11. The modeled and loss for V-H polarization at 11GHz in building1.

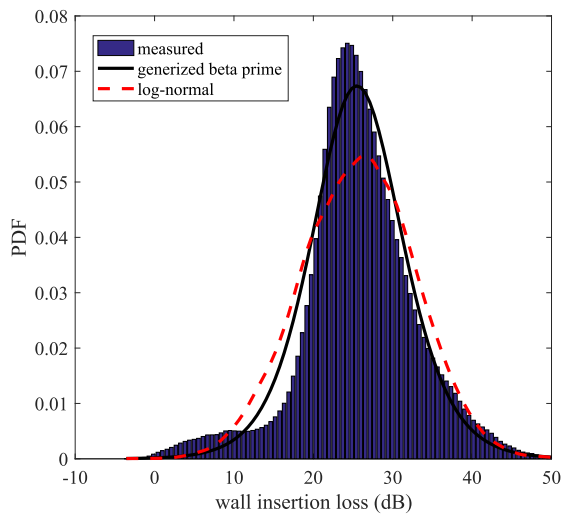


FIGURE 10. The modeled and the measured PDF of the wall insertion loss for V-V polarization at 11GHz in building1.

TABLE 7. The statistics of the K-S tests and chi-square test for different polarizations at 3.5GHz.

building	Distribution	V-V		V-H	
		K-S	Chi-square	K-S	Chi-square
building1	Proposed	0.01	0.03	0.02	0.01
	Lognormal	0.03	0.42	0.04	0.15
building2	Proposed	0.015	0.017	0.028	0.021
	Lognormal	0.022	0.10	0.035	0.13
building3	Proposed	0.021	0.22	0.03	0.04
	Lognormal	0.051	2.62	0.05	0.18

TABLE 8. The statistics of the K-S tests and chi-square test for different polarizations at 6GHz.

building	Distribution	V-V		V-H	
		K-S	Chi-square	K-S	Chi-square
building1	Proposed	0.014	0.015	0.022	0.072
	Lognormal	0.035	0.20	0.039	2.04
building2	Proposed	0.011	0.01	0.015	0.15
	Lognormal	0.028	0.69	0.027	1.31
building3	Proposed	0.022	0.12	0.020	0.26
	Lognormal	0.037	1.09	0.035	1.87

TABLE 9. The statistics of the K-S tests and chi-square test for different polarizations at 11GHz.

building	Distribution	V-V		V-H	
		K-S	Chi-square	K-S	Chi-square
building1	Proposed	0.031	0.89	0.017	0.053
	Lognormal	0.044	1.10	0.024	0.15
building2	Proposed	0.029	0.94	0.03	0.24
	Lognormal	0.045	1.97	0.05	1.18
building3	Proposed	0.02	0.22	0.02	0.09
	Lognormal	0.05	2.62	0.04	0.87

In the Chi-square test, the statistic is defined by

$$\chi^2 = \sum_{j=1}^k \frac{(O_j - E_j)^2}{E_j} \quad (15)$$

where O_j is the sampled value of the measured CDF, E_j is the sampled value of the fitted CDF, and k is the last sample along the CDF.

In the K-S test, the statistic is defined by

$$D = \sup_x |F_n(x) - F(x)| \quad (16)$$

where \sup_x is the supremum of the set of the distances. $F_n(x)$ and $F(x)$ are the measured CDF and the fitted CDF, respectively.

Obviously, both in the K-S test and Chi-square test, the smaller statistic corresponds a better fit between the measured and modeled results.

Table 7-9 compares the statistics of the K-S tests and chi-square test for different frequencies and polarizations. The table shows that the proposed model outperforms the Lognormal model in terms of the smaller statistics in the K-S and Chi-square tests. The reason is that Nakagami distribution fits the small scale fading better than the log-normal distribution in the indoor-indoor channel.

Therefore, we can conclude that the IWIL can be modeled by the generalized beta prime distribution. The proposed model can be used in the small cell network for future work. For example, this model will be useful for the path loss assessment and then the outage probability for any point in the cell can be determined. Thus, the wireless coverage prediction will be more accurate, especially at the edge of the cells.

V. CONCLUSION

In this paper, a novel closed-form and stochastic IWIL model is presented. The IWIL is found to possess a generalized beta prime distribution. The modeled PDF, expectation and standard deviation of the IWIL are derived. The expectation decreases as the m_2 -factor increases for a constant Ω_1/Ω_2 and it tends to Ω_1/Ω_2 for large m_2 -factor. The standard deviation decreases as the m -factors of both links increase for a fixed m_1/m_2 .

In order to validate the accuracy of the proposed model, several wall insertion loss measurements are conducted for the V-V and V-H polarizations at 3GHz, 6GHz, 11GHz band. The PDF of the measured and modeled IWIL is utilized as the evaluation metric. The PDF of Log-normal distribution is also compared. Both K-S and Chi-square tests are exploited to determine the goodness of the fitting. Both of the tests show that the proposed model gives smaller statistics than the Log-normal model, due to the fact that Nakagami distribution fits the small scale fading better than the log-normal distribution in the indoor-indoor channel.

The proposed model can be employed for the small cell design, such as the link budget calculation, the indoor wireless coverage and the electromagnetic compatibility analysis, in the future 5G communication system.

APPENDIX A

PROOF OF THE PDF OF THE WALL INSERTION LOSS

If Y and Z are two independent Gamma distributed variables, $Y \sim \text{Gamma}(\alpha_1, \beta_1)$, $Z \sim \text{Gamma}(\alpha_2, \beta_2)$, then the PDFs of the variables Y, Z are

$$f_Y(y) = \frac{\beta_1^{\alpha_1} y^{\alpha_1-1} e^{-\beta_1 y}}{\Gamma(\alpha_1)} \quad y > 0, \alpha_1 > 0, \beta_1 > 0 \quad (17)$$

$$f_Z(z) = \frac{\beta_2^{\alpha_2} z^{\alpha_2-1} e^{-\beta_2 z}}{\Gamma(\alpha_2)} \quad z > 0, \alpha_2 > 0, \beta_2 > 0 \quad (18)$$

where $\Gamma(\cdot)$ is the gamma function [15].

Thus, the CDF of the variable $X = Y/Z$ can be calculated as

$$F_X(x) = \int_0^\infty f_Z(z) \int_0^{zx} f_Y(y) dy dz \quad (19)$$

The PDF of the variable X can be obtained by taking the derivative of the equation (19) with respect to x ,

$$f_X(x) = \int_0^\infty z f_Z(z) f_Y(zx) dz \quad (20)$$

Putting the equations (17) and (18) into (20), we can get

$$f_X(x) = \frac{\beta_2^{\alpha_2} \beta_1^{\alpha_1} x^{\alpha_1-1}}{\Gamma(\alpha_1)\Gamma(\alpha_2)} \int_0^\infty z^{\alpha_1+\alpha_2-1} e^{(-\beta_2-\beta_1 x)z} dz \quad (21)$$

In order to calculate the integration in equation (21), we denote $(\beta_2 + \beta_1 x)z = u$, then (21) can be written as

$$f_X(x) = \frac{(\frac{\beta_1}{\beta_2}x)^{\alpha_1-1} \cdot (1 + \frac{\beta_1}{\beta_2}x)^{-(\alpha_1+\alpha_2)}}{\frac{\beta_2}{\beta_1}} \cdot \frac{\Gamma(\alpha_1 + \alpha_2)}{\Gamma(\alpha_1)\Gamma(\alpha_2)} \quad (22)$$

Considering the relationship between gamma function and beta function,

$$B(\alpha_1, \alpha_2) = \frac{\Gamma(\alpha_1)\Gamma(\alpha_2)}{\Gamma(\alpha_1 + \alpha_2)} \quad (23)$$

and taking it into (22), we can get

$$f_X(x) = \frac{(\frac{\beta_1}{\beta_2}x)^{\alpha_1-1} \cdot (1 + \frac{\beta_1}{\beta_2}x)^{-(\alpha_1+\alpha_2)}}{\frac{\beta_2}{\beta_1} \cdot B(\alpha_1, \alpha_2)} \quad (24)$$

Substitute $m_1, m_2, m_1/\Omega_1$, and m_2/Ω_2 for the parameters $\alpha_1, \alpha_2, \beta_1$ and β_2 in (15) respectively, then the PDF of the wall insertion loss can be derived as the equation (5).

APPENDIX B

PROOF OF THE EXPECTATION AND STANDARD DEVIATION OF THE WALL INSERTION LOSS

The mean of IWIL can be calculated as

$$E(I_{loss}) = \int_0^\infty x f_{I_{loss}}(x) dx \quad (25)$$

Substituting (10) into (25), we have

$$E(I_{loss}) = \frac{\Omega_1}{\Omega_2} \cdot \frac{m_2}{m_1} \cdot \frac{B(m_1 + 1, m_2 - 1)}{B(m_1, m_2)} \quad m_2 > 2 \quad (26)$$

Considering the relationship between gamma function and beta function, equation (26) can be rewritten as

$$E(I_{loss}) = \frac{\Omega_1}{\Omega_2} \cdot \frac{m_2}{m_1} \cdot \frac{\Gamma(m_1 + 1) \cdot \Gamma(m_2 - 1)}{\Gamma(m_1) \cdot \Gamma(m_2)} \quad m_2 > 1 \quad (27)$$

Owing to the property of gamma function

$$\Gamma(x + 1) = x\Gamma(x) \quad (28)$$

We can simplify (27) further to

$$E(I_{loss}) = \frac{\Omega_1}{\Omega_2} \cdot \frac{m_2}{m_2 - 1} \quad m_2 > 1 \quad (29)$$

In order to calculate the standard deviation of IWIL, the second-order central moment is calculated as

$$E(I_{loss}^2) = \int_0^\infty x^2 f_{I_{loss}}(x) dx \quad (30)$$

Substituting (10) into (27), the second-order central moment can be expanded as

$$E(I_{loss}^2) = \frac{\Omega_1}{\Omega_2} \cdot \frac{m_2}{m_1} \cdot \frac{B(m_1 + 2, m_2 - 2)}{B(m_1, m_2)} \quad m_2 > 2 \quad (31)$$

According to the equation (23) and (28), we can write

$$E(I_{loss}^2) = (\frac{m_2}{m_1} \cdot \frac{\Omega_1}{\Omega_2})^2 \cdot \frac{m_1(m_1 + 1)}{(m_2 - 2)(m_2 - 1)} \quad m_2 > 2 \quad (32)$$

Then the standard deviation can be obtained as

$$\text{Std}(I_{\text{loss}}) = \sqrt{E(I_{\text{loss}}^2) - [E(I_{\text{loss}})]^2} \quad (33)$$

Putting the results (29) and (32) into (33), we can get

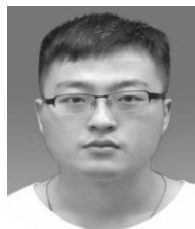
$$\text{Std}(I_{\text{loss}}) = \frac{\Omega_1}{\Omega_2} \cdot \frac{m_2}{m_1} \cdot \sqrt{\frac{m_1(m_1 + m_2 - 1)}{(m_2 - 2)(m_2 - 1)^2}} \quad m_2 > 2 \quad (34)$$

ACKNOWLEDGMENT

The authors are also indebted to Mr. Yan Qin and Mr. Xiao-lei Wang, China Telecommunication Technology Laboratory (CTTL), for their help and assistance in the channel measurement.

REFERENCES

- [1] S. Chen and J. Zhao, "The requirements, challenges, and technologies for 5G of terrestrial mobile telecommunication," *IEEE Commun. Mag.*, vol. 52, no. 5, pp. 36–43, May 2014.
- [2] V. Jungnickel et al., "The role of small cells, coordinated multipoint, and massive MIMO in 5G," *IEEE Commun. Mag.*, vol. 52, no. 5, pp. 44–51, May 2014.
- [3] R. J. C. Bultitude, "Measurement, characterization and modeling of indoor 800/900 MHz radio channels for digital communications," *IEEE Commun. Mag.*, vol. CM-25, no. 6, pp. 5–12, Jun. 1987.
- [4] T. S. Rappaport, "Characterization of UHF multipath radio channels in factory buildings," *IEEE Trans. Antennas Propag.*, vol. 37, no. 8, pp. 1058–1069, Aug. 1989.
- [5] X. Zhao, S. Geng, and B. M. Coulibaly, "Path-loss model including LOS-NLOS transition regions for indoor corridors at 5 GHz [wireless corner]," *IEEE Trans. Antennas Propag.*, vol. 55, no. 3, pp. 217–223, Jun. 2013.
- [6] J. Zhu, H. Wang, and W. Hong, "Large-scale fading characteristics of indoor channel at 45-GHz band," *IEEE Antennas Wireless Propag. Lett.*, vol. 14, pp. 735–738, 2015.
- [7] D. Devasirvatham, "A comparison of time delay spread and signal level measurements within two dissimilar office buildings," *IEEE Trans. Antennas Propag.*, vol. AP-35, no. 3, pp. 319–324, Mar. 1987.
- [8] A. Muqaibel, A. Safaai-Jazi, A. Attiya, B. Woerner, and S. Riad, "Path-loss and time dispersion parameters for indoor UWB propagation," *IEEE Trans. Wireless Commun.*, vol. 5, no. 3, pp. 550–559, Mar. 2006.
- [9] G. R. Maccartney, T. S. Rappaport, S. Sun, and S. Deng, "Indoor office wideband millimeter-wave propagation measurements and channel models at 28 and 73 GHz for ultra-dense 5G wireless networks," *IEEE Access*, vol. 3, pp. 2388–2424, 2015.
- [10] T. S. Rappaport and C. D. McGillem, "UHF fading in factories," *IEEE J. Sel. Areas Commun.*, vol. 7, no. 1, pp. 40–48, Jan. 1989.
- [11] A. F. Abouraddy and S. M. Elnoubi, "Statistical modeling of the indoor radio channel at 10 GHz through propagation measurements. I. Narrow-band measurements and modeling," *IEEE Trans. Veh. Technol.*, vol. 49, no. 5, pp. 1491–1497, Sep. 2000.
- [12] E. Vinogradov, W. Joseph, and C. Oestges, "Measurement-based modeling of time-variant fading statistics in indoor peer-to-peer scenarios," *IEEE Trans. Antennas Propag.*, vol. 63, no. 5, pp. 2252–2263, May 2015.
- [13] A. A. M. Saleh and R. Valenzuela, "A statistical model for indoor multipath propagation," *IEEE J. Sel. Areas Commun.*, vol. SAC-5, no. 2, pp. 128–137, Feb. 1987.
- [14] D. Cassioli, M. Z. Win, and A. F. Molisch, "The ultra-wide bandwidth indoor channel: From statistical model to simulations," *IEEE J. Sel. Areas Commun.*, vol. 20, no. 6, pp. 1247–1257, Aug. 2002.
- [15] X. Wu et al., "60-GHz millimeter-wave channel measurements and modeling for indoor office environments," *IEEE Trans. Antennas Propag.*, vol. 65, no. 4, pp. 1912–1924, Apr. 2017.
- [16] T. M. Schafer, J. Maurer, J. von Hagen, and W. Wiesbeck, "Experimental characterization of radio wave propagation in hospitals," *IEEE Trans. Electromagn. Compat.*, vol. 47, no. 2, pp. 304–311, May 2005.
- [17] N. Moraitis and P. Constantinou, "Indoor channel measurements and characterization at 60 GHz for wireless local area network applications," *IEEE Trans. Antennas Propag.*, vol. 52, no. 12, pp. 3180–3189, Dec. 2004.
- [18] G. Hwang, K. Shin, S. Park, and H. Kim, "Measurement and comparison of Wi-Fi and super Wi-Fi indoor propagation characteristics in a multi-floored building," *J. Commun. Netw.*, vol. 18, no. 3, pp. 476–483, Jun. 2016.
- [19] T. B. Gibson and D. C. Jenn, "Prediction and measurement of wall insertion loss," *IEEE Trans. Antennas Propag.*, vol. 47, no. 1, pp. 55–57, Jan. 1999.
- [20] W. Braun and U. Dersch, "A physical mobile radio channel model," *IEEE Trans. Veh. Technol.*, vol. 40, no. 2, pp. 472–482, May 1991.
- [21] A. Bekker, J. Roux, and T. Pham-Gia, "The type I distribution of the ratio of independent 'Weibullized' generalized beta-prime variables," *Stat. Papers*, vol. 50, no. 20, pp. 323–338, Mar. 2009.
- [22] F. W. J. Olver, D. W. Lozier, R. F. Boisvert, and C. W. Clark, *NIST Handbook of Mathematical Functions*. Cambridge, U.K.: Cambridge Univ. Press, 2010.
- [23] A. Muqaibel, A. Safaai-Jazi, A. Bayram, A. M. Attiya, and S. M. Riad, "Ultrawideband through-the-wall propagation," *IEEE Proc. Microw. Antennas Propag.*, vol. 152, no. 6, pp. 581–588, Dec. 2005.
- [24] Y. Yu, P.-F. Cui, W.-J. Lu, Y. Liu, and H.-B. Zhu, "Off-body radio channel impulse response model under hospital environment: Measurement and modeling," *IEEE Commun. Lett.*, vol. 20, no. 11, pp. 2332–2335, Nov. 2016.
- [25] W. Feller, *An Introduction to Probability Theory and its Applications*, vol. 1, 3rd ed. Hoboken, NJ, USA: Wiley, 1968.
- [26] H. Hashemi, "The indoor radio propagation channel," *Proc. IEEE*, vol. 81, no. 7, pp. 943–968, Jul. 1993.
- [27] F. J. Massey, Jr., "The Kolmogorov-Smirnov test for goodness of fit," *J. Amer. Stat. Assoc.*, vol. 46, no. 253, pp. 68–78, 1951.
- [28] W. G. Cochran, "The X^2 test of goodness of fit," *Ann. Math. Stat.*, vol. 23, pp. 315–345, Sep. 1952.



YANG LIU was born in Wuxi, China, in 1988. He received the Ph.D. degree in communication and information system from the Key Laboratory of Wireless Communication, Nanjing University of Posts and Telecommunications, Nanjing, China, in 2016. He is currently a Lecturer with the Institute of IOT Engineering, Jiangnan University, Wuxi. He has authored and co-authored over ten technical papers published in peer-reviewed international journals and conference proceedings.

His research interests include the wireless propagation and wireless channel modeling.



YU YU was born in Nanjing, China, in 1990. He received the B.E. degree in communication engineering from the Nanjing University of Posts and Telecommunications, Nanjing, in 2012. His research interests include wireless propagation and wireless channel modeling.



QIONG WU was born in Xuzhou, China, in 1986. He received the Ph.D. degree in information and communication engineering from the National Mobile Communication Research Laboratory, Southeast University, Nanjing, China, in 2016. He is currently a Lecturer with the Institute of IOT Engineering, Jiangnan University, Wuxi. His research interests include the medium access control in vehicular ad hoc networks.



ZHENG-QUAN LI was born in Enshi, China, in 1974. He received the B.S. degree from Jilin University in 1998, the M.S. degree from the University of Shanghai in 2000, and the Ph.D. degree from Shanghai Jiaotong University in 2003. He is currently a Professor with the Institute of IOT Engineering, Jiangnan University, Wuxi. His research interests include wireless channel modeling, channel estimation, and massive MIMO coding.



HONG-BO ZHU was born in Yangzhou, China, in 1956. He is currently the standing Director of the Chinese Institute of Electronics and the Director of the Jiangsu Key Laboratory of Wireless Communications, Nanjing University of Posts and Telecommunications. He has authored and co-authored over 100 journal papers and over 60 invention patents authorized. In the past five years, he has undertaken over 30 projects at the national, provincial and ministerial level. His research interests include wireless communications, Internet of Things, and EMC.

...



WEN-JUN LU (M'12) was born in Jiangmen, China, in 1978. He received B.E. and Ph.D. degrees in communication engineering and electrical engineering from the Nanjing University of Posts and Telecommunications (NUPT), Nanjing, China, in 2001 and 2007, respectively. He has been a Lecturer from 2007 to 2009, an Associate Professor from 2009 to 2013, and since 2013, he has been a Professor with the Jiangsu Key Laboratory of Wireless Communications, NUPT.

He is the Translator of the Chinese version *The Art and Science of Ultra Wideband Antennas* (by H. Schantz). He has authored the book *Antennas: Concise Theory, Design and Applications* (in Chinese). He has authored and co-authored over 100 technical papers published in peer-reviewed international journals and conference proceedings. His research interests include antenna theory, wideband antennas and arrays. He has been serving as an Editorial Board Member of International Journal of RF and Microwave Computer-Aided Engineering, since 2014. He was the recipient of the Exceptional Reviewers Award of the IEEE TRANSACTIONS ON ANTENNAS AND PROPAGATION, in 2016, Award of New Century Excellent Talents in Universities from the Ministry of Education of China in 2012, and the Nomination Award of Top-100 Outstanding Ph.D. Dissertation of China in 2009. He was also the co-recipient of other six scientific and technological awards granted by the Jiangsu Province, Chinese Institute of Electronics, and Chinese Institute of Communications, respectively.